IEICE TRANS. COMMUN., VOL.E89–B, NO.12 DECEMBER 2006

PAPER Special Section on Software Defined Radio Technology and Its Applications

# Influence of ADC Nonlinearity on the Performance of an OFDM Receiver

Manabu SAWADA[†,††a)], Hiraku OKADA[††*], Takaya YAMAZATO[†††], *and* Masaaki KATAYAMA[†††], *Members*

**SUMMARY** This paper discusses the influence of the nonlinearity of analog-to-digital converters (ADCs) on the performance of orthogonal frequency division multiplexing (OFDM) receivers. We evaluate signal constellations and bit error rate performances while considering quantization errors and clippings. The optimum range for an ADC input amplitude is found as a result of the trade-off between quantization error and the effects of clipping. In addition, it is shown that the peak-to-average power ratio (PAPR) of the signal is not a good measure of the bit error rate (BER) performance, since the largest peaks occur only with very low probabilities. The relationship between the location of a subcarrier and its performance is studied. As a result, it is shown that the influence of the quantization error is identical for all subcarriers, while the effects of clipping depend on the subcarrier frequency. When clipping occurs, the BER performance of a subcarrier near the center frequency is worse than that near the edges.

*key words: OFDM, ADC, nonlinearity, quantization error, clipping*

## 1. Introduction

Orthogonal frequency division multiplexing (OFDM), which can adaptively modify its coding, signal constellations, and assigned power for each subcarrier according to the change of communication environment, has attracted much attention due to its design flexibility and high frequency usage. Because of this flexibility, OFDM is one of the most important modulation schemes in software defined radio systems.

In the OFDM scheme, a high-rate data stream is split into a number of lower-rate streams and transmitted over a number of subcarriers. As a property of multi-carrier signals, the OFDM signal has large fluctuation in its amplitude. Thus OFDM systems should have large dynamic range and high linearity. The main cause of nonlinearity at a transmitter is the power amplifier. In order to reduce the nonlinear distortion caused by the amplifier, the "predistortion technique" and the "clipping and filtering technique" have been discussed in [1]–[4].

At a receiver of OFDM signals, the nonlinearity of the analog-to-digital converter (ADC), which is a key device in a software defined radio, should be considered. When the amplitude of an OFDM signal at the input of the ADC is too large, the signal is distorted by the clipping as in Case 1 of Fig. 1. If the signal is too small as in Case 2, the quantization errors dominate the performance.

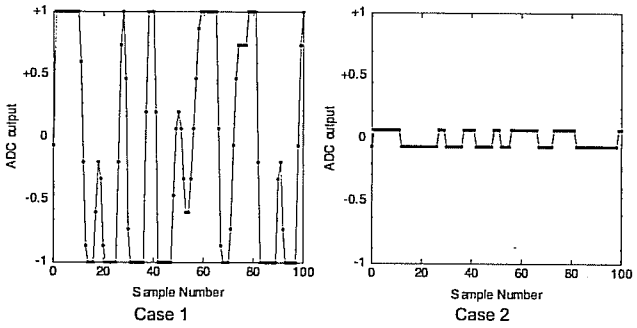


**Fig. 1** Outputs of the ADC.

The influence of the nonlinearity of the ADC in an OFDM receiver is discussed in [5], [6]. In [5], the bit error rate (BER) performance is evaluated while giving consideration to the quantization errors to determine the parameters of the ADC. In [6], the BER performance of an OFDM system is evaluated when clipping occurs in the signal.

Since the number of quantization bits in an ADC is finite, there is a trade-off between quantization error and clipping when an analog signal is quantized by the ADC. This paper evaluates the BER performance by taking both quantization errors and the effects of clipping into account to clarify the results of this trade-off.

For better understanding of the effects of the ADC, we investigate the influences of quantization error and clipping on the constellation at each subcarrier of a received OFDM signal. We also examine whether the PAPR is a suitable measure of sensitivity to the nonlinearity of an ADC in BER performance. In addition, we describe not only the overall BER performance but also the BER performances of individual subcarriers.

## 2. System Model

Figure 2 shows the equivalent low-pass model of the OFDM receiver discussed in this paper. We assume that the ideal filter, whose equivalent noise bandwidth is $N/T$, limits noise power without any influence on the signal. All the blocks of the receiver except the ADCs are assumed to be linear, and the sampling timing is assumed to have no jitter. There-

Manuscript received March 6, 2006.
Manuscript revised June 29, 2006.

[†]The author is with Research Laboratories, DENSO CORPORATION, Yokosuka-shi, 239-0847 Japan.
[††]The authors are with the Department of Electrical Engineering and Computer Science, Graduate School of Engineering, Nagoya University, Nagoya-shi, 464-8603 Japan.
[†††]The authors are with EcoTopia Science Institute, Nagoya University, Nagoya-shi, 464-8603 Japan.
*Presently, with Niigata University.
a) E-mail: msawada@rlab.denso.co.jp

DOI: 10.1093/ietcom/e89–b.12.3250

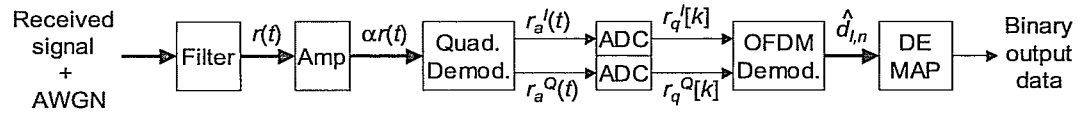


**Fig. 2** Receiver model.

fore, the equivalent low-pass model at the filter output can be expressed as

$$r(t) = s(t) + n_o(t), \tag{1}$$

where $s(t)$ is a signal component and $n_o(t)$ is a noise component. The signal component $s(t)$ is expressed as

$$s(t) = \sqrt{\frac{1}{N}} \sum_{l=-\infty}^{\infty} \sum_{n=0}^{N-1} d_{l,n} \exp\left\{j2\pi \frac{n}{T}(t - lT)\right\} \cdot p(t - lT), \tag{2}$$

where $d_{l,n}$ is the $2^U$-ary QAM symbol at the $l$-th OFDM symbol duration on the $n$-th subcarrier [7]. The OFDM symbol duration is $T$, and the number of subcarriers is $N$. The pulse shape of an OFDM symbol is defined as

$$p(t) = \begin{cases} 1 & 0 \le t < T \\ 0 & \text{otherwise.} \end{cases} \tag{3}$$

Let the mean square value of $d_{l,n}$ be unity. Then the power of the signal is

$$\frac{1}{T} E\left[\int_{lT}^{(l+1)T} |s(t)|^2 dt\right] = 1, \tag{4}$$

and the average energy per bit is

$$E_b = E\left[\frac{1}{NU}\int_{lT}^{(l+1)T} |s(t)|^2 dt\right] = \frac{T}{NU}, \tag{5}$$

where $E[\ ]$ denotes expectation or ensemble average.

Let the two-sided spectral density of AWGN at the input of the filter be $N_0$. The noise component $n_o(t)$ in Eq. (1) is a complex Gaussian variable with zero mean and variance $\sigma_n^2$, where

$$\sigma_n^2 = N_0 \frac{N}{T}. \tag{6}$$

The filter output $r(t)$ is amplified with gain $\alpha$ and fed to the quadrature demodulator. Although the gain $\alpha$ may be automatically controlled according to the input level in practical systems, the following discussion assumes a fixed gain in order to provide information on the target range of $\alpha$.

The outputs of the quadrature demodulator are fed to the pair of ADCs. The ADC inputs for in-phase (Ich) and quadrature-phase (Qch) are represented as

$$r_a^I(t) = \Re[\alpha r(t)] \tag{7}$$

and

$$r_a^Q(t) = \Im[\alpha r(t)]. \tag{8}$$

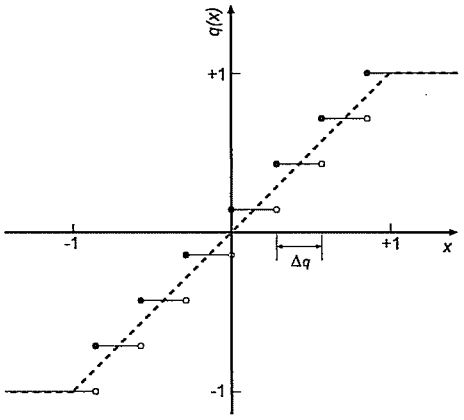


**Fig. 3** $q(x)$ for $M = 3$.

In each ADC, the input signal is sampled at every $T_q$ seconds. The sampling interval $T_q$ is represented as

$$T_q = \frac{T}{K_d} = \frac{T}{\eta N}, \tag{9}$$

where $K_d$ is the number of samples in an OFDM symbol duration at each ADC with the over-sample factor $\eta$. The full-scale range (FSR) of the ADC input is normalized to arrange $\pm 1$. The corresponding ADC outputs at $t = kT_q$ are represented as

$$r_q^I[k] = q\left(r_a^I(kT_q)\right) \tag{10}$$

and

$$r_q^Q[k] = q\left(r_a^Q(kT_q)\right). \tag{11}$$

In these equations $q(x)$ is expressed as

$$q(x) = \begin{cases} 1 & x \ge 1 \\ \left\lfloor \frac{x}{\Delta_q} \right\rfloor \Delta_q + \frac{\Delta_q}{2} & -1 \le x < 1 \\ -1 & x < -1, \end{cases} \tag{12}$$

where $\lfloor x \rfloor$ is the maximum integer that does not exceed $x$. Since the FSR is $\pm 1$, the step size of the $M$ bit quantizer is expressed as

$$\Delta_q = \frac{2}{2^M - 1}. \tag{13}$$

Figure 3 shows $q(x)$ for $M = 3$.

The distortion caused by the ADC can be defined as follows.

$$\begin{cases} e_q^I[k] = r_a^I(kT_q) - r_q^I[k] \\ e_q^Q[k] = r_a^Q(kT_q) - r_q^Q[k] \end{cases} \tag{14}$$

The behavior of the distortion depends on the level of the ADC input. If the ADC input amplitude is in the FSR, i.e.

$$|r_a(kT_q)| < 1 + \frac{\Delta_q}{2}, \tag{15}$$

the magnitude of the distortion (the quantization error) is upper-limited as

$$|e_q[k]| < \frac{\Delta_q}{2}. \tag{16}$$

The clipping occurs when the ADC input amplitude is out of the FSR, i.e.

$$|r_a(kT_q)| > 1 + \frac{\Delta_q}{2}. \tag{17}$$

In this case,

$$|e_q[k]| > \frac{\Delta_q}{2}. \tag{18}$$

In Eq. (15)–(18), the superscript I or Q is omitted.

In the OFDM demodulator, the samples $r_q^I[k]$ and $r_q^Q[k]$ in an OFDM duration are converted into $N$ corresponding QAM symbols using a $K_d$-point FFT. The output of the FFT for the $l$-th OFDM symbol duration and the $n$-th subcarrier is expressed as

$$\tilde{d}_{l,n} = \frac{1}{K_d} \sum_{k=lK_d}^{(l+1)K_d-1} \left(r_q^I[k] + jr_q^Q[k]\right) \exp\left\{-j2\pi \frac{kn}{K_d}\right\}. \tag{19}$$

This output $\tilde{d}_{l,n}$ is then normalized as

$$\hat{d}_{l,n} = \frac{1}{D}\tilde{d}_{l,n}, \tag{20}$$

where $D$ is the average value of $|\tilde{d}_{l,n}|$ and expressed as

$$D = \frac{1}{NL} \sum_{l=0}^{L-1} \sum_{n=0}^{N-1} |\tilde{d}_{l,n}|. \tag{21}$$

The OFDM demodulator output $\hat{d}_{l,n}$ is demapped to a set of binary data.

## 3. Signal Constellation

Figure 4 shows the constellation at the OFDM demodulator output obtained by computer simulation for $L = 150$ symbols of $N = 64$ subcarriers: there are $L \cdot N = 9600$ points in this figure. QPSK is used for subcarrier modulation, i.e. $U = 2$. As a result of the quantization error and the clipping, the received symbols fluctuate in the constellation even though the channel is noiseless.

As a measure of the fluctuation in the signal constellations, let us define the variance of demodulated symbols in the constellation as

$$\sigma^2 = \frac{1}{NL} \sum_{l=0}^{L-1} \sum_{n=0}^{N-1} \left(\hat{d}_{l,n} - d_{l,n}\right)^2. \tag{22}$$

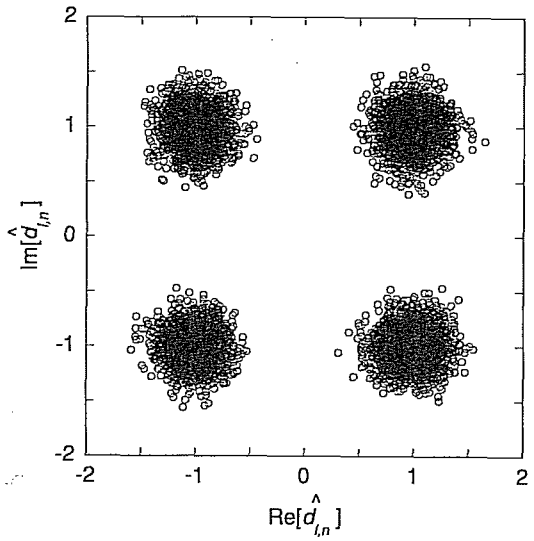


**Fig. 4** Constellation at the OFDM demodulator output (noiseless, QPSK/OFDM, $N = 64, M = 8, \eta = 4, \alpha = 1, L = 150$).

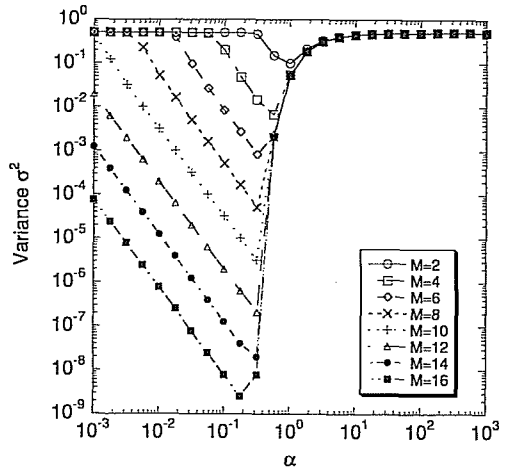


**Fig. 5** Variance $\sigma^2$ of $\hat{d}_{l,n}$ (noiseless, QPSK/OFDM, $N = 64, \eta = 4$).

For example, the variance $\sigma^2$ is about 0.05 in Fig. 4. In order to indicate the influence of $\alpha$, the variance $\sigma^2$ is calculated by simulation. Figure 5 shows the variances $\sigma^2$ of $\hat{d}_{l,n}$ with $N = 64$ for various resolutions $M$. For each $M$, there is an optimum value for $\alpha$ in this figure. When the gain $\alpha$ is smaller than the optimum value, the signal is distorted by the quantization error. On the other hand, when the gain $\alpha$ is larger than the optimum value, the signal is distorted by the clipping.

## 4. Bit Error Rate Performance

In this section, BERs are evaluated by computer simulation. According to the rule of thumb, the number of bits for BER simulation should be on the order of 10/BER [8]. In order to satisfy this requirement, we employ $1.28 \times 10^8$ bits for simulation while BER $\geq 10^{-7}$.

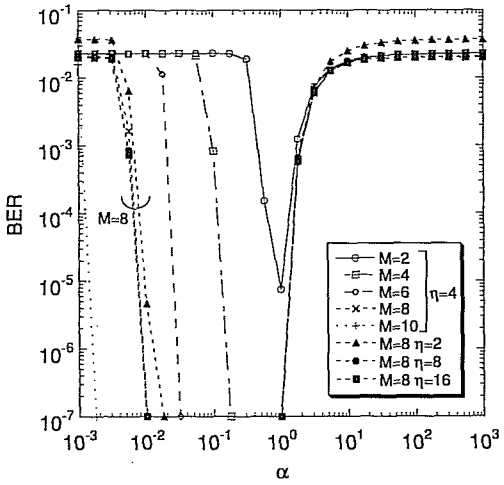


Fig. 6 BER performance of a QPSK/OFDM signal (noiseless, $N = 64$).

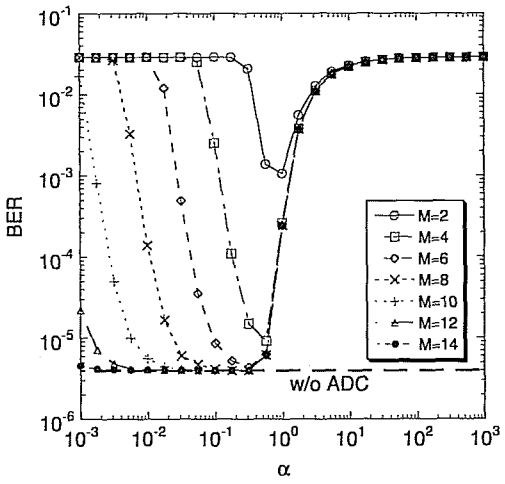


Fig. 7 BER performance of a QPSK/OFDM signal ($E_b/N_0 = 10$ dB, $N = 64$).

### 4.1 BER Performance in Noiseless Channel

Figure 6 shows the relationship between BER performance of a QPSK/OFDM signal received without noise and its amplitude (amplifier gain $\alpha$) for various values of $M$.

Figure 6 shows that the errors occur in the received bits even without channel noise when $\alpha$ is too small or too large. It is also shown that there is a range of the value for $\alpha$ when $M \geq 4$, where BER $\leq 10^{-7}$. This range of $\alpha$ is wider when $M$ is larger. In addition, it is noteworthy that BER can not be lower than $10^{-6}$, even without channel noise if the number of quantization bits $M$ is too small (=2).

In addition, Fig. 6 shows that the BER is not sensitive to the over-sample factor $\eta$, and especially for $\eta \geq 4$ all BER curves overlap each other. Thus in the following numerical examples, $\eta = 4$ is used.

### 4.2 BER Performance in AWGN Channel

Figure 7 shows the BER performance of a QPSK/OFDM signal with AWGN ($E_b/N_0 = 10$ dB). The influence of $\alpha$ tends to be similar to that in the noiseless case shown in Fig. 6. In Fig. 7, because of the channel noise, there is an error floor at BER $= 4 \times 10^{-6}$, which is the BER without the influence of the ADCs. The range of $\alpha$, where this error floor can be achieved, is narrower than the optimum range in Fig. 6, where BER $\leq 10^{-7}$.

Figure 8 shows BER performance as a function of $E_b/N_0$. There are error floors when $\alpha = 0.1$ and $M = 2$ or 4. These are caused by the quantization error, while an error floor at $\alpha = 1$ and $M = 2$ is the result of clipping.

### 4.3 Influence of PAPR on BER Performance

The PAPR is often used as a measure of amplitude fluctuation of OFDM signals, and a signal with a large PAPR is assumed to be sensitive to the nonlinearity of the system. In a conventional OFDM system without coding, PAPR is

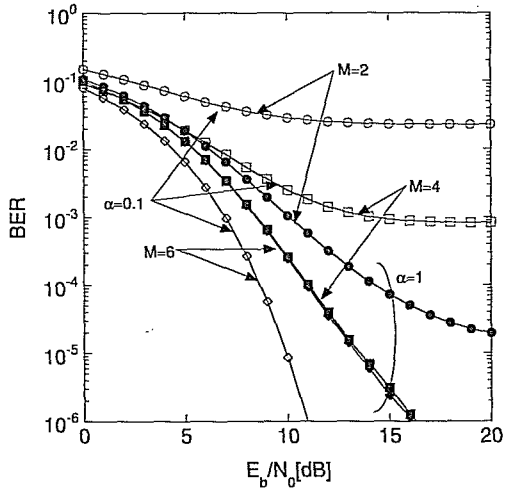


Fig. 8 BER performance of a QPSK/OFDM signal ($N = 64$).

proportional to $N$. Thus it can be supposed that a signal with large $N$ has worse performance under the nonlinearity of ADCs. But in reality, the BER performance does not depend so much on $N$ as seen in Fig. 9, which shows the BER performance of a QPSK/OFDM signal for different $N$. The reason of this is that the PAPR is not a measure of the probability of the peak amplitude. In order to clarify how often the peak occurs, the cumulative complementary distribution function (CCDF) of the instantaneous power ($|s(t)|^2$) of a QPSK/OFDM signal is shown in Fig. 10. The CCDF for the Gaussian distribution of the same variance is also shown in the figure. Since the average power of the signal $s(t)$ is unity, the PAPR is the same as the peak power of the OFDM signal, which is equal to $N$. Thus at $|s(t)|^2 = N$, CCDF is zero.

In Fig. 10, it is clear that the distributions of the instantaneous powers of an OFDM signal are almost the same for large $N$, and they approach the Gaussian distribution, according to the central limit theorem. This observation indi-

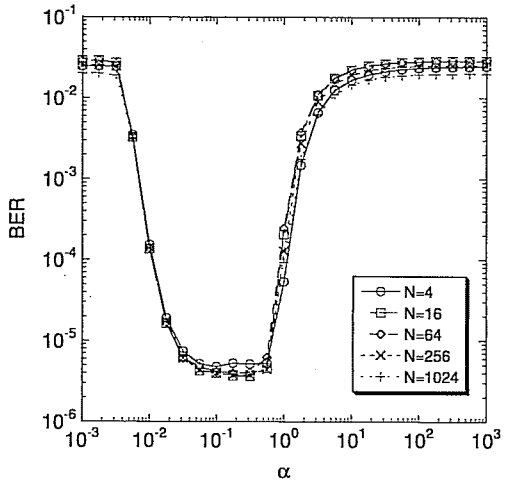


**Fig. 9** BER performance of a QPSK/OFDM signal for different $N$ ($E_b/N_0 = 10$ dB, $M = 8$).

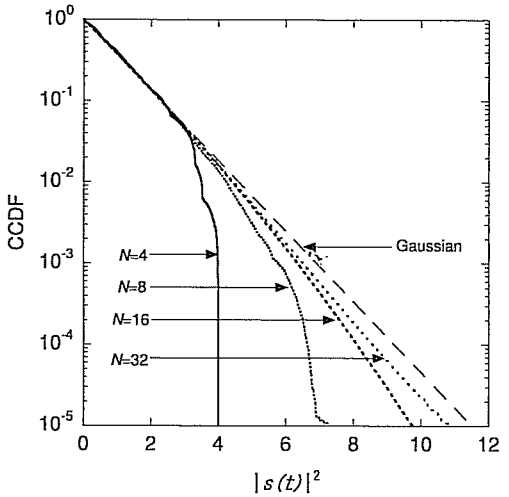


**Fig. 10** CCDF of the instantaneous power ($|s(t)|^2$) of a QPSK/OFDM signal.

cates that the peak power, which is equal to $N$, occurs with very low probability, especially if $N$ is large. In fact, the probability for $|s(t)|^2 \geq 2$ is less than 20% for all $N$, and the probability for $|s(t)|^2 \geq 5$ is less than 1% if $N \geq 8$. Since the distribution of the instantaneous power is almost the same regardless of $N$, the BER curves in Fig. 9 nearly overlap each other.

### 4.4 BER Performance of Individual Subcarriers

Figure 11 shows the BER performance of individual subcarriers of a QPSK/OFDM signal with $N = 64$ subcarriers. For this figure, $2 \times 10^6$ bits for each subcarrier ($1.28 \times 10^8$ bits in total) are tested to evaluate BER. This satisfies the rule of thumb on simulation bits, if BER is the order of $10^{-5}$. The horizontal axis shows the index $n_s$ expressed as

$$n_s = n - \frac{N}{2}, \tag{23}$$

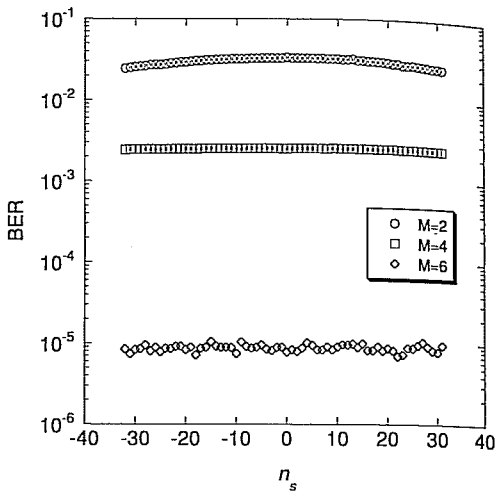


(a) $\alpha = 0.1$.

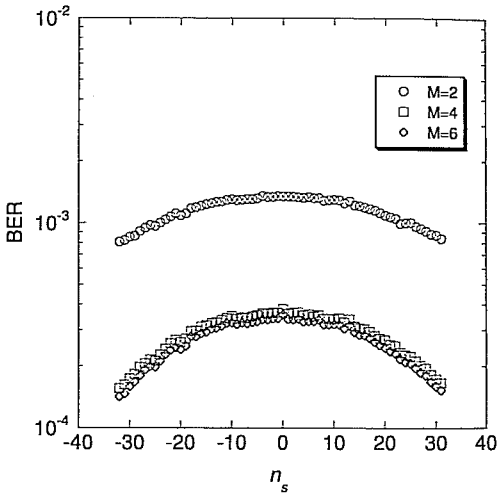


(b) $\alpha = 1$.

**Fig. 11** BER performance of individual subcarriers of a QPSK/OFDM signal ($E_b/N_0 = 10$ dB, $N = 64$).

where $n$ is the subcarrier number of Eq. (2). Fig. 11(a) shows the performance with $\alpha = 0.1$, in which the quantization error dominates the performance, while clipping dominates the performance in Fig. 11(b) with $\alpha = 1$.

In Fig. 11(a), the BER performances for all subcarriers are almost the same, while in Fig. 11(b), the BER performance of the center frequency area is worse than that of the edge frequency area.

It is known that the influence of the intermodulation distortion caused by nonlinear amplification of an OFDM signal is larger for subcarriers in the center frequency area than that in the edge frequency area [9]. This fact explains the feature shown in Fig. 11(b). When $\alpha$ and thus signal amplitude is large, the clipping dominates performance rather than the quantization error. In this situation, the input/output characteristic of the ADC ($q(x)$) can be approximated by a soft limiter shown by the dashed line in Fig. 3, and the effect of the distortion of this nonlinear amplification becomes larger in the center frequency area.

### 4.5 BER Performances of 16QAM/OFDM and 64QAM/OFDM Signals

In the above discussion, QPSK ($U = 2$) is employed for subcarrier modulation. In this subsection we evaluate the BER performances of modulation using large $U$ with amplitude modulation, i.e., 16QAM ($U = 4$) and 64QAM ($U = 6$). Figures 12 and 13 show the BER performances of 16QAM/OFDM and 64QAM/OFDM signals, respectively. The values of $E_b/N_0$ in Figs. 7, 12 and 13 are set so that the BER performances without the influence of the ADCs are almost the same.

Comparing Figs. 7, 12 and 13, we can find that the influence of $\alpha$ on BER performance brings us to the same conclusion: the existence of an optimum range of $\alpha$. Moreover, the ranges for a given $M$ are almost the same for these three subcarrier modulation schemes.

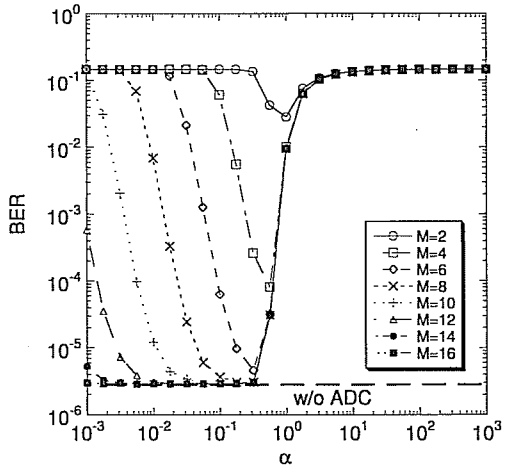


**Fig. 12** BER performance of a 16QAM/OFDM signal ($E_b/N_0 = 14$ dB, $N = 64$).

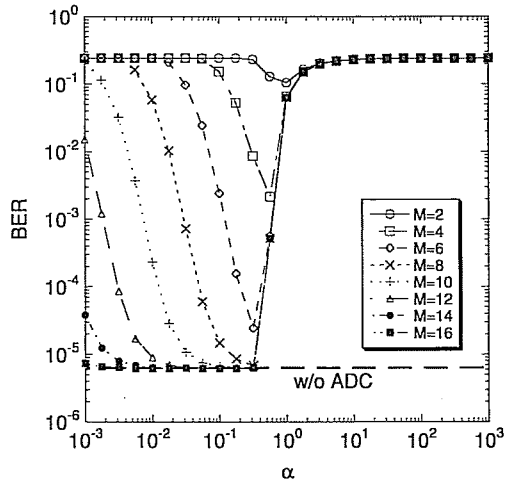


**Fig. 13** BER performance of a 64QAM/OFDM signal ($E_b/N_0 = 18$ dB, $N = 64$).

## 5. Conclusion

In this paper, we discussed the influence of the nonlinearity of the ADC in the receiver on the performance of a received OFDM signal. The performance was discussed in terms of the variance of signal points on the signal constellations and BER. We also presented the optimum range for an ADC input amplitude as well as the trade-off between the quantization error and clipping. This optimum range can be used as the target output of an automatic gain controlled (AGC) amplifier. In addition, we showed that this optimum range for an ADC input amplitude is wider when the number of quantization bits is larger. This means that system designers can reduce the cost of an AGC amplifier when higher-cost ADCs are used in the OFDM receiver.

Furthermore, we showed that the influence of the PAPR on the BER performance is little and the BER performance is dominated by the average power rather than by PAPR. This means that using PAPR as a measure of sensitivity is not always suitable for the nonlinearity of an ADC. Furthermore, the relationship between the BER performance of individual subcarriers and the locations of the subcarriers was clarified. As a result, the influence of the quantization error proved to be identical for all subcarriers, but BER under clipping was found to be frequency dependent. When clipping occurs at the ADC input, the BER performance of the subcarriers in the center frequency area is worse than that in the edge frequency area. This paper confirms that the influence of clipping at the ADC input tends to be similar to that of nonlinear amplification. The discussion was made on QPSK/OFDM, and the validity of the argument was also confirmed for 16QAM/OFDM and 64QAM/OFDM. Consequently, we found that the differences in the subcarrier modulation schemes only affect the required quantization bits.

#### References

[1] H.W. Kang, Y.S. Cho, and D.H. Youn, "On compensating nonlinear distortions of an OFDM system using an efficient adaptive predistorter," IEEE Trans. Commun., vol.47, no.4, pp.522–526, April 1999.
[2] X. Li and L.J. Cimini, Jr., "Effect of clipping and filtering on the performance of OFDM," IEEE Commun. Lett., vol.2, no.5, pp.131–133, May 1998.
[3] L.J. Cimini, Jr. and N.R. Sollenberger, "Peak-to-average power ratio reduction of an OFDM signal using partial transmit sequences," IEEE Commun. Lett., vol.4, no.3, pp.86–88, March 2000.
[4] T. Fujii and M. Nakagawa, "Adaptive clipping level control for OFDM peak power reduction using clipping and filtering," IEICE Trans. Fundamentals, vol.E85-A, no.7, pp.1647–1655, July 2002.
[5] J.C. de M. Garcia and A.G. Armada, "Effects of bandpass sigma-delta modulation on OFDM signals," IEEE Trans. Consum. Electron., vol.45, no.2, pp.318–326, May 1999.
[6] A. Moschitta and D. Petri, "Wideband communication system sensitivity to overloading quantization noise," IEEE Trans. Instrum. Meas., vol.52, no.4, pp.1302–1307, Aug. 2003.
[7] R. van Nee and R. Prasad, OFDM for Wireless Multimedia Communications, Artech House, 2000.
[8] M.C. Jeruchim, "Techniques for estimating the bit error rate in the simulation of digital communication system," IEEE J. Sel. Areas

Commmun., vol.SAC-2, no.1, pp.153–170, Jan. 1984.
[9] M.R.D. Rodrigues and J.J. O'Reilly, "On the distribution of the intermodulation distortion in OFDM communication systems," Proc. London Communications Symposium 2001, pp.87–90, London, UK, Sept. 2001.
[10] M. Sawada, H. Okada, T. Yamazato, and M. Katayama, "Influence of the nonlinearity of the ADC in an OFDM receiver," 10th International OFDM-Workshop, pp.220–224, Aug. 2005.

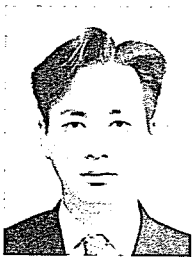

**Manabu Sawada** was born in Kanazawa, Japan in 1969. He received the B.S. and M.S. degrees from Nagoya University, Japan in 1992 and 1994, respectively. In 1994, he joined Research Laboratories, Nippondenso Co., Ltd. (now DENSO CORPORATION). His current research interests include mobile communication systems and intelligent transport systems. He is a member of IEEE and SITA.

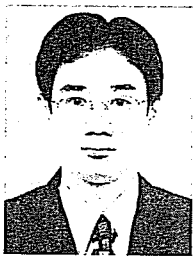

**Hiraku Okada** received the B.S., M.S. and Ph.D. degrees in Information Electronics Engineering from Nagoya University, Japan in 1995, 1997 and 1999, respectively. From 1997 to 2000, he was a research fellow of the Japan Society for the Promotion of Science. In 1999, he was a visiting researcher in Department of Electronics and Electrical Engineering, the University of Edinburgh. From 2000 to 2006, he was an Assistant Professor at Nagoya University, Japan. Since 2006, he has been an Associate Professor in the Center for Transdisciplinary Research, Niigata University, Japan. His current research interests include packet radio communications, multimedia traffic, wireless multihop networks, and CDMA technologies. He received the Inose Science Award in 1996, and the IEICE Young Engineer Award in 1998. Dr. Okada is a member of IEEE and SITA.

**Takaya Yamazato** was born in Okinawa, Japan in 1964. He received the B.S. and M.S. degrees from Shinshu University, Nagano, Japan, in 1988 and 1990, respectively, and received the Ph.D. degree from Keio University, Yokohama, Japan, in 1993, all in Electrical Engineering. From 1993 to 1998, he was an Assistant Professor in the Department of Information Electronics, Nagoya University, Japan. From 1997 to 1998, he was a visiting researcher of the Research Group for RF Communications, Department of Electrical Engineering and Information Technology, University of Kaiserslautern. Form 1998 to 2004, he was an Associate Professor in the Center for Information Media Studies, Nagoya University, Japan. Since 2004, he has been with the EcoTopia Science Institute, Nagoya Univeristy, Japan. His research interests include sensor networks, satellite and mobile communication systems, CDMA, and joint source-channel coding. Dr. Yamazato received the IEICE Young Engineer Award in 1995 and the IEEE Communication Society 2006 The Best Tutorial Paper Award in 2006. He is a member of IEEE and SITA.

**Masaaki Katayama** was born in Kyoto, Japan in 1959. He received the B.S., M.S. and Ph.D. degrees from Osaka University, Japan in 1981, 1983, and 1986, respectively, all in Communication Engineering. He was an Assistant Professor at Toyohashi University of Technology from 1986 to 1989, and a Lecturer at Osaka University from 1989 to 1992. In 1992, he joined Nagoya University as an associate professor, and has been a professor since July 2001. He also had been working at the College of Engineering of the University of Michigan from 1995 to 1996 as a visiting scholar. His current research interests are on the physical and media-access layers of radio communication systems. His current research projects include, Software Defined Radio, Reliable Robust Radio Control with multi-dimensional coding and signal processing, Power-Line Communications, Visible Light Communications, Next Generation Mobile Communications, and Satellite Communications. He received the IEICE (was IECE) Shinohara Memorial Young Engineer Award in 1986. Dr. Katayama is a member of SITA, IEICE, Reliablility Engineering Associaton of Japan. He is also a senior member of IEEE.